# Cascadability of Optical 3R Regeneration for NRZ Format Investigated in Recirculating Loop Transmission Over Field Fibers

Masaki Funabashi, Zuqing Zhu, Zhong Pan, Bo Xiang, Loukas Paraschis, David L. Harris, and S. J. B. Yoo, *Senior Member, IEEE*

***Abstract*—This letter demonstrates optical 3R regeneration in 10-Gb/s nonreturn-to-zero field transmission. The 3R regenerator utilizes semiconductor-optical-amplifier-based Mach–Zehnder interferometer wavelength converters, a synchronous modulator, and a Fabry–Pérot filter to realize optical 3R regeneration including all-optical clock recovery. The cascadablity of the 3R regenerator is investigated in recirculating loop transmission experiments with various regeneration spacings up to 462 km (corresponding to an input optical signal-to-noise ratio (OSNR) of 22 dB). Transmission with the 3R regenerator shows significant performance improvement over that without 3R regeneration. A 66-km-spaced 3R regeneration with a 33-dB input OSNR achieves 1000-hop cascaded error-free transmission (66 000 km in distance) with no hop-to-hop power penalties. A 264-km-spaced 3R regeneration with a 25-dB input OSNR also achieves 100-hop cascaded transmission (26 400 km in distance) with a bit-error-rate error floor at $\sim 1 \times 10^{-8}$.**

***Index Terms*—All-optical clock recovery, Fabry–Pérot filter (FPF), field fiber, nonreturn-to-zero (NRZ), optical regeneration.**

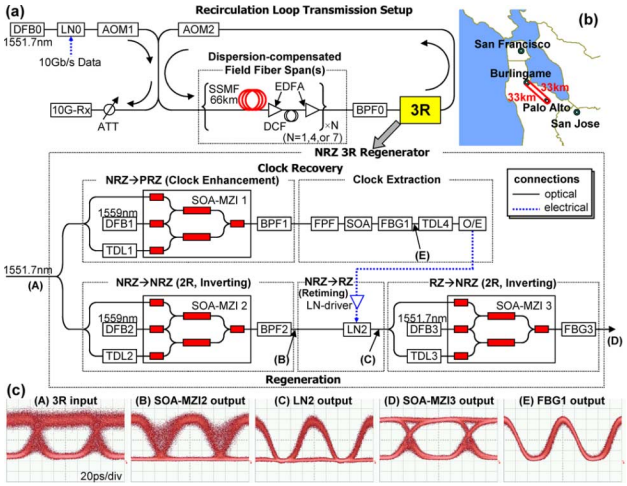


Fig. 1. (a) Experimental setup. (b) Field fiber map. (c) Eye diagrams at the locations (A)–(E) when $L_R = 264$ km and the lap number is Lap2.

## I. Introduction

OPTICAL signals after fiber transmission undergo various distortions due to the impairments caused by noise, attenuation, and fiber dispersion and nonlinearity. Optical signal regeneration is a promising technology for advanced optical networking in overcoming these impairments by restoring the signal quality [1]. While numerous publications reported on optical 3R regeneration in well-controlled laboratory environments [2]–[5], only a few have demonstrated a field trial of optical 2R [6] or 3R regeneration [7]. Moreover, the majority of previous studies on 3R regeneration techniques employ a return-to-zero (RZ) format [2]–[5], [7], and only a few have discussed 3R regeneration for the most commonly used nonreturn-to-zero (NRZ) format [8], [9]. The main advantage of optical regeneration is to enhance transmission distance by cascading regenerators, and recirculating loop setups are typically used to investigate the cascadability [2]–[5]. Reference [5] also investigated the regeneration spacing dependence of the cascadability for the RZ format in a laboratory environment. This letter demonstrates 3R regeneration for a 10-Gb/s NRZ signal in a recirculating loop transmission over field fiber links. The utilization of semiconductor-optical-amplifier-based Mach–Zehnder interferometer (SOA-MZI) wavelength converters, a Fabry–Pérot filter (FPF), and a synchronous modulator realizes 3R regeneration, as well as all-optical clock recovery from the NRZ signal [10]–[12]. The cascadability of the 3R regenerator is investigated with various regeneration spacings and optical signal-to-noise ratios (OSNRs).

## II. Experimental Setup

Fig. 1(a) and (b) shows the experimental setup and the field fiber map. The recirculating loop transmission setup enables cascadability evaluation of an inline 3R regenerator. As a transmission line, up to seven sets of field fibers were used. The field fibers are standard single-mode fibers in a loop-back configuration between Burlingame and Palo Alto. Each field fiber span has a round-trip length of 66 km, followed by a two-stage erbium-doped fiber amplifier with a dispersion-compensating fiber (DCF) in its middle stage. The 3R regenerator was located after a predetermined number ($N$) of the fiber spans ($N = 1, 4,$ or 7; corresponding to a regeneration spacing ($L_R$) of 66, 264, or 462 km). After the first, fourth, and seventh span, residual dispersion values were within ±30 ps/nm, and OSNR degraded to 33, 25, and 22 dB, respectively, from the initial value of 45 dB

Manuscript received May 9, 2006; revised July 25, 2006. This work was supported in part by Furukawa Electric, Cisco System URP Program, and in part by the National Science Foundation under NSF 0335301 and NSF 9986665.

M. Funabashi is with the Department of Electrical and Computer Engineering, University of California, Davis, CA 95616 USA, and also with Furukawa Electric Co., Ltd., Yokohama 220-0073, Japan.

Z. Zhu, Z. Pan, B. Xiang, and S. J. B. Yoo are with the Department of Electrical and Computer Engineering, University of California, Davis, CA 95616 USA (e-mail: yoo@ece.ucdavis.edu).

L. Paraschis is with Advanced Technology, Core Routing, Cisco Systems, San Jose, CA 95134 USA.

D. L. Harris is with Advanced Technology Labs, Next Gen Transport, Sprint, Burlingame, CA 94010 USA.

Color versions of Figs. 1–4 are available online at http://ieeexplore.ieee.org.

Digital Object Identifier 10.1109/LPT.2006.883222

1041-1135/$20.00 © 2006 IEEE

(0.1-nm bandwidth). To reduce OSNR degradation while maintaining the linear optical transmission regime, the input power level to each field fiber and DCF fiber is set moderately high at 5 and 0 dBm, respectively.

The 3R regenerator consists of a clock recovery part and a signal regeneration part. In the clock recovery part, the SOA-MZI1 in the noninverting differential operation mode generates an RZ pulse at every rising and falling edge in the incoming NRZ signal, providing NRZ to pseudo-RZ (PRZ) conversion. This conversion strengthens the weak 10-GHz clock components in the NRZ signal. The subsequent FPF, with a free spectral range of 10 GHz and a finesse of 100, filters out the enhanced clock components and recovers an optical clock signal [13], which contains strong pattern-dependent amplitude variations. The limiting amplification effect of the subsequent gain-saturated SOA reduces the amplitude variations [13] and the narrow spectral filtering effect in the fiber Bragg grating filter (FBG1) forces the recovered optical clock signal to a smooth sinusoidal waveform and reduces pattern-dependent variations involving higher frequency components. However, the optical recovered clock signal still exhibits the amplitude variations when the word length is long. Here, the experiment has adopted a short pseudorandom bit sequence of $2^7 - 1$ to focus our attention on the regeneration spacing dependence of the 3R regenerator cascadability. The recovered optical clock signal is converted into an electrical signal that synchronously modulates the data stream for retiming. In the signal regeneration part, the two SOA-MZIs operating in the inverting mode provide 2R regeneration. The synchronous modulator LN2, driven by the optical-to-electrical-converted recovered clock signal, performs retiming, as well as NRZ-to-RZ conversion. The SOA-MZI3 followed by the FBG3 converts the RZ format back to the NRZ format. Although both of the SOA-MZIs have differential signal inputs, they basically operate in the single-arm condition.

## III. Experimental Results

Fig. 1(c) shows the eye diagrams measured at the locations (A)–(E) in the setup, when $L_R$ is 264 km and the lap number is Lap2. The eye diagram (A) at the 3R input is distorted in both the amplitude and time domains through the field fiber transmission. The inverting-mode SOA-MZI2 clamps the mark-level amplitude noise in the incoming signal and produces the well-defined space level in (B). The subsequent synchronous modulator LN2, driven by the optical recovered clock (E), reduces the timing jitter noise, as seen in (C). Subsequent to the other inverting-mode SOA-MZI3, the overall power transfer function provides flat responses for both the mark and space levels. The flat responses contribute to enhanced nonlinearity of the transfer function, suppressing the noise on the mark and space levels effectively. The eye diagram (D) shows clear eye openings and an improved extinction ratio. These results are in agreement with [14], which suggested the importance of high nonlinearity of the transfer function and a high extinction ratio in order to obtain better cascadability.

Fig. 2(a)–(c) shows eye diagrams after the various recirculating loop transmission experiments when the regeneration spacings are (a) 66, (b) 264, and (c) 462 km, respectively. Removing the "NRZ 3R regenerator" block in Fig. 1(a), hereafter referred to as the "1R" case, causes the eye openings to

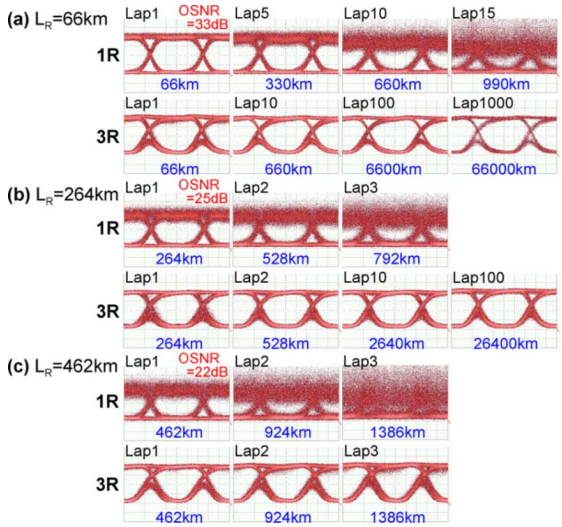


Fig. 2. Eye diagrams after recirculating loop transmission without 3R (1R) and with 3R regeneration (3R). $L_R$ is (a) 66, (b) 264, and (c) 462 km.

reduce as the lap number increases, which is more apparent in the amplitude domain. With 3R regeneration, however, the eye diagrams sustain open eyes up to a much larger lap number than that without 3R regeneration. When $L_R$ is 66 or 264 km, almost identical eye diagrams are obtained from Lap1 to each final lap. When $L_R$ is 462 km, the amplitude noise accumulations on the mark level are so severe that they remain in some slight form even after 3R regeneration.

Fig. 3(a)–(c) shows bit-error-rate (BER) curves. When $L_R$ is 66 km (33-dB input OSNR, Fig. 3(a)), the power penalty without 3R regeneration steadily increases with the lap number, showing 0.3, 0.6, and 1.6 dB at a BER of $10^{-9}$ for Lap1, Lap2, and Lap5, respectively, from the back-to-back (B-to-B) result as a base. On the other hand, the BER curves with 3R regeneration overlap with each other without an error floor, and the power penalties from the B-to-B are less than 1 dB for all cases. The hop-to-hop power penalties are almost negligible up to Lap1000, which corresponds to a transmission distance of 66 000 km. When $L_R$ is 264 km Fig. 3(b), the 1R-Lap1 curve shows a 1.8-dB power penalty, due to the reduced OSNR of 25 dB. After 3R, however, the power penalty is improved to 0.6 dB, which is comparable to that of the 3R_Lap1 case in Fig. 3(a). The BER curves are almost identical up to Lap10 before they start to show bending. Transmission up to Lap100 (26 400 km in distance) has been achieved with a BER error floor at $\sim 1 \times 10^{-8}$. For $L_R = 462$ km [Fig. 3(c)], the 1R_Lap1 curve shows bending and a power penalty higher than 4 dB, due to severe signal degradation (22-dB OSNR). The 3R results are much better than the 1R results, but an error floor at $1 \times 10^{-8}$ develops after Lap3 (1386 km in distance).

Fig. 4 shows the $Q$-factor as a function of transmission distance. The upper horizontal axis shows the corresponding cumulative loss, estimated from the average fiber span loss. The $Q$-factor is calculated from a measured BER versus threshold voltage curve. In the case of 1R only, the $Q$-factor continues to decrease with the distance from the initial value of 20 dB at B-to-B. With 3R regeneration, the $Q$-factors for $L_R = 66$ and 264 km start with slightly smaller values, around

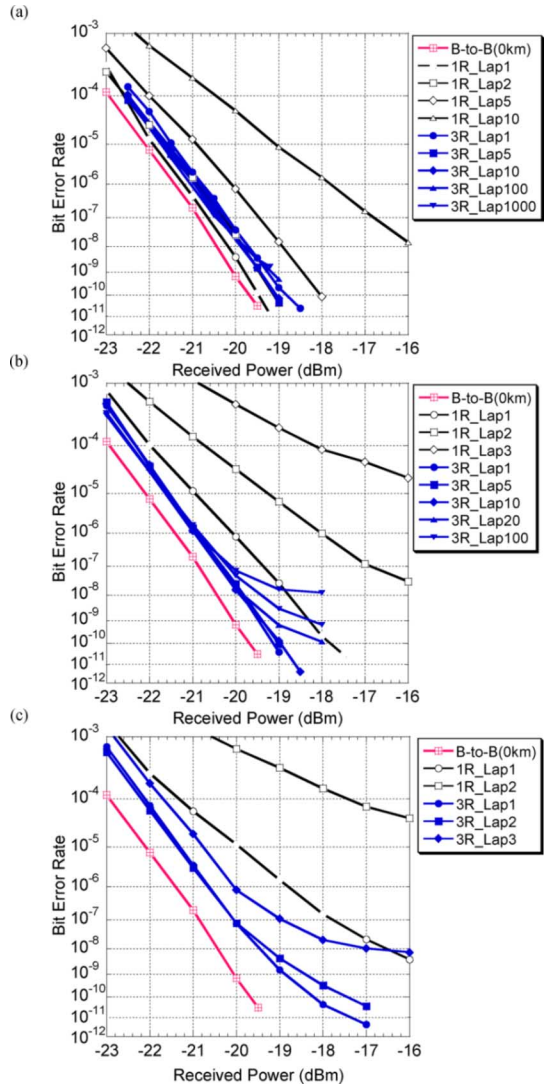


Fig. 3. BER curves for $L_R$ of (a) 66, (b) 264, and (c) 462 km.

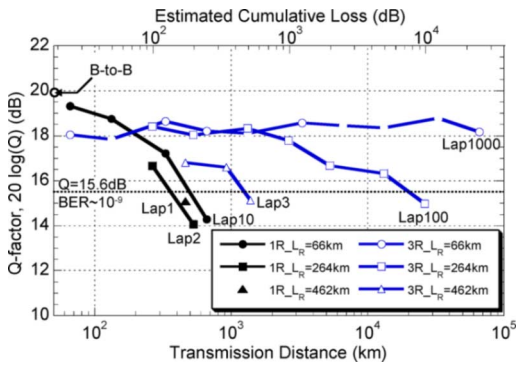


Fig. 4. $Q$-factor versus transmission distance.

18 dB, however they remain almost constant up to 66 000 and 2640 km, respectively. These results are consistent with the trends observed in the eye diagrams and the BER curves, indicating that a shorter regeneration spacing can maintain a high $Q$-factor up to a larger number of cascade stages. In other words, if requirements for the distance and $Q$-factor are not stringent, an extended regeneration spacing and a low input OSNR are acceptable for more cost-effective implementation. Although the eye, BER, and $Q$-factor results indicate that the amplitude noise accumulation is the dominant degradation mechanism for the 3R performance, the timing jitter noise accumulations also appear in the eye diagrams, especially with the longer regeneration spacings. The recovered clock signal degradations and the timing jitter accumulations can be resulting from the transfer of the amplitude noise in the incoming NRZ signal to the timing jitter noise of the PRZ signal during the NRZ-to-PRZ conversion.

## IV. Conclusion

We have demonstrated cascaded 3R regeneration of 10-Gb/s NRZ signals using recirculating loop transmission over field fibers. The inline 3R regenerator considerably improves the signal quality, the cascadability, and the transmission distance, compared to those without 3R regeneration. A 66-km-spaced 3R regeneration with a 33-dB input OSNR has achieved 1000-hop cascaded error-free 66 000-km transmission with no hop-to-hop power penalties. A 264-km-spaced 3R regeneration with a 25-dB input OSNR has exhibited 100-hop cascaded 26 400-km transmission with a BER error floor at $\sim 1 \times 10^{-8}$.

## References

[1] O. Leclerc, B. Lavigne, E. Balmefrezol, P. Brindel, L. Pierre, D. Rouvillain, and F. Seguineau, "Optical regeneration at 40 Gb/s and beyond," *J. Lightw. Technol.*, vol. 21, no. 11, pp. 2779–2790, Nov. 2003.

[2] G. Raybon *et al.*, "40 Gbit/s pseudo-linear transmission over one million kilometers," in *Proc. OFC 2002*, Anaheim, CA, Paper FD10.

[3] B. Lavigne, P. Guerber, P. Brindel, E. Balmefrezol, and B. Dagens, "Cascade of 100 optical 3R regenerators at 40 Gbit/s based on all-active Mach Zehnder interferometers," in *Proc. ECOC'01*, 2001, vol. 3, pp. 290–291.

[4] Z. Zhu, M. Funabashi, Z. Pan, L. Paraschis, and S. J. B. Yoo, "10 000-hop cascaded in-line all-optical 3R regeneration to achieve 1 250 000-km 10-Gb/s transmission," *IEEE Photon. Technol. Lett.*, vol. 18, no. 5, pp. 718–720, Mar. 1, 2006.

[5] G. Gavioli, V. Mikhailov, B. Thomsen, and P. Bayvel, "Investigation of transmission with cascaded all-optical 3R regenerators and variable inter-regenerator spacing," *Electron. Lett.*, vol. 41, pp. 146–148, 2005.

[6] D. Chen *et al.*, "Triple 640 km cascade of tunable all optical regenerators in a 10 Gb/s WDM field trial over 160 km per span distance in MCI's metro network," in *Proc. ECOC'05*, 2005, vol. 3, pp. 405–406.

[7] M. Yagi *et al.*, "Field trial of optical 3R regenerator over installed cable," in *Proc. ECOC'05*, 2005, vol. 4, pp. 975–976.

[8] D. Chiaroni *et al.*, "New 10 Gbit/s 3R NRZ optical regenerative interface based on semiconductor optical amplifiers for all-optical networks," in *Proc. ECOC'97*, 1997, vol. 5, pp. 41–44.

[9] H. S. Chung, R. Inohara, K. Nishimura, and M. Usami, "40-Gb/s NRZ wavelength conversion with 3R regeneration using an EA modulator and SOA polarization-discriminating delay interferometer," *IEEE Photon. Technol. Lett.*, vol. 18, no. 2, pp. 337–339, Jan. 15, 2006.

[10] C. Kim, I. Kim, X. Li, and G. Li, "All-optical clock recovery of NRZ data at 40 Gbit/s using Fabry–Perot filter and two-section gain-coupled DFB laser," *Electron. Lett.*, vol. 39, pp. 1456–1458, 2003.

[11] G. Contestabile, M. Presi, N. Calabretta, and E. Ciaramella, "All-optical clock recovery from 40 Gbit/s NRZ signal based on clock line enhancement and sharp periodic filtering," *Electron. Lett.*, vol. 40, pp. 1361–1362, 2004.

[12] J. Slovak, C. Bornholdt, J. Kreissl, S. Bauer, M. Biletzke, M. Schlak, and B. Sartorius, "Bit rate and wavelength transparent all-optical clock recovery scheme for NRZ-coded PRBS signals," *IEEE Photon. Technol. Lett.*, vol. 18, no. 7, pp. 844–846, Apr. 1, 2006.

[13] G. T. Kanellos, L. Stampoulidis, N. Pleros, T. Houbavlis, D. Tsiokos, E. Kehayas, H. Avramopoulos, and G. Guekos, "Clock and data recovery circuit for 10-Gb/s asynchronous optical packets," *IEEE Photon. Technol. Lett.*, vol. 15, no. 11, pp. 1666–1668, Nov. 2003.

[14] F. Ohman and J. Mork, "Modeling of bit error rate in cascaded 2R regenerators," *J. Lightw. Technol.*, vol. 24, no. 2, pp. 1057–1063, Feb. 2006.